Aquaculture 613 (2026) 743299

Contents lists available at ScienceDirect

Aquaculture

journal homepage: www.elsevier.com/locate/aquaculture

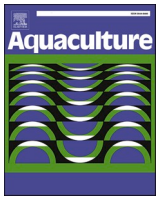

An integrated modelling approach for the stocking optimisation of a commercial-scale salmon-kelp IMTA system

Amalia Krupandan [a,*], Lynne Falconer [a], Julie Maguire [b], Trevor Telfer [a]

[a] Institute of Aquaculture, University of Stirling, Stirling, Scotland FK9 4LA, UK
[b] Bantry Marine Research Station Ltd., Gearhies, Bantry, Co. Cork P75 AX0, Ireland

ARTICLE INFO

Dataset link: Data relating to publication: Salmon cage wastes increase kelp growth in commercial scale open coast integrated multi-trophic aquaculture system (Original data)

Keywords:
Aquaculture planning
Bioremediation
Decision support
Coastal resource management
Integrated multi-trophic aquaculture
Nutrient transfer
Sustainability

ABSTRACT

Coastal Integrated Multi-Trophic Aquaculture (IMTA) systems, which combine the cultivation of extractive species like sugar kelp (*Saccharina latissima*) with fed species such as Atlantic salmon (*Salmo salar*), are often suggested as a way to diversify farm production and reduce environmental impact. However, commercial-scale IMTA faces challenges in synchronizing nutrient transfer and uptake between species, influenced by environmental and production factors. This study presents an integrated modelling approach to optimize stocking strategies in a commercial-scale salmon-kelp IMTA system located in Bantry Bay, Ireland. The modelling approach combines a salmon growth model, hydrography, and a re-parameterised Dynamic Energy Budget model for kelp growth. The study evaluates different stocking scenarios to assess their impact on nutrient cycling and biomass yields. Results from the simulations indicate that extending the kelp growing season considerably enhances kelp biomass yield and nitrogen assimilation, with the potential to mitigate up to 3.07 % of salmon-derived nitrogen waste under the scenarios investigated for this farm. The findings highlight the importance of timing in kelp stocking and suggest that early deployment could improve nutrient removal efficiency. This integrated modelling framework provides valuable insights for optimizing IMTA systems by improving species management and nutrient synchronisation at farm level.

1. Introduction

Coastal Integrated Multi-Trophic Aquaculture (IMTA) involves growing extractive species like sugar kelp (*Saccharina latissima)* in the waste stream of fed species like Atlantic salmon (*Salmo salar*) (Chopin et al., 2001, 2012; Reid et al., 2013). However, thus far, commercial scale IMTA remains limited, with scalability constraints and management complexity representing significant barriers to widespread adoption (Hughes and Black, 2016; Hossain et al., 2022; Sickander and Filgueira, 2022). Scalability challenges arise from the need to develop extractive species operations at scales that provide meaningful environmental mitigation, often constrained by limited available space close to existing farms where extractive species can be effectively cultivated (Broch et al., 2013; Brager et al., 2016). Additional logistical challenges emerge considering the scale of post-harvest processing needed (Stévant and Rebours, 2021). This is compounded by biological complexities inherent in coordinating multi-species systems such as coordinating harvest and processing operations for diverse products with distinct seasonal cycles (Alexander and Hughes, 2017; Kleitou et al., 2018; Sickander and Filgueira, 2022). IMTA systems must synchronize species that grow and respond to environmental factors at different rates and can often lead to seasonal mismatch in production (Broch et al., 2013; Handå et al., 2013; Fossberg et al., 2018; Nederlof et al., 2022). In a salmon farm, feeding strategies will usually focus on fish growth, health, welfare and product quality (Mock et al., 2021; Hvas et al., 2024), but in a salmon-kelp IMTA, the nutrient waste must also align with the uptake capacity of kelp, which fluctuates due to seasonal changes in temperature, light availability, and hydrodynamics (Hurd et al., 2014; Roleda and Hurd, 2019). If salmon produce nutrients at a time when kelp growth is limited, the efficiency of the IMTA system will be decreased (Nederlof et al., 2022). Conversely, if seasonal factors were suitable for high kelp growth but nutrient supply is insufficient, full production potential of the kelp may not be realized. The interaction of these processes makes it difficult for producers to determine the best practice for species management, stocking and harvest strategies.

Predictive models can provide important information for aquaculture planning and management (Falconer et al., 2023), with potential to help decision-makers with the coordination of different species in

* Corresponding author.
E-mail address: amalia.krupandan@stir.ac.uk (A. Krupandan).

https://doi.org/10.1016/j.aquaculture.2025.743299
Received 14 May 2025; Received in revised form 16 September 2025; Accepted 12 October 2025
Available online 14 October 2025

commercial scale IMTA setup and operation. However, effective modelling of salmon-kelp IMTA systems requires integrating multiple biological and environmental processes, each governed by distinct modelling approaches. Modern fish growth models have advanced from general bioenergetic frameworks to more detailed nutrient-based models that explicitly track the ingestion, assimilation, and excretion of specific nutrients, offering a more precise estimate of nutrient release into the surrounding environment (Dumas et al., 2010; Nobre et al., 2019; Soares et al., 2023). While substantial progress has been made in modelling fish metabolism, kelp growth models have lagged due to the complexity of photoautotrophic physiology, which requires consideration of carbon acquisition, light utilization, and nutrient uptake strategies (Gordillo, 2012; Hurd et al., 2014). Recent advancements, such as Dynamic Energy Budget (DEB) models, have improved the mechanistic representation of kelp growth by explicitly tracking carbon and nitrogen assimilation, making these models more generalizable across varying environmental conditions (Lavaud et al., 2020; Venolia et al., 2020). Yet, the effectiveness of IMTA depends not only on species-specific growth dynamics but also on the environmental transport of nutrients, which is highly variable in open-water systems. Hydrodynamic models play a critical role in determining the availability of nutrients for extractive species by simulating the effects of currents and stratification on nutrient dispersion (Reid et al., 2020; Nederlof et al., 2022). Conceivably, an integrated approach, combining models for both species and connectivity, could help address some of the questions related to IMTA species management and synchronisation in coastal and open-water locations.

The overall aim of this study was to develop and use a modelling approach to investigate the effect of different salmon-kelp stocking strategies on kelp growth and bioremediation potential in a coastal salmon-kelp IMTA system. The first objective was to develop and test an integrated modelling approach capable of simulating key interactions between salmon production, hydrodynamic nutrient transport, and kelp growth. The second objective was to use this model to compare different IMTA scenarios to assess how varying stocking densities and production schedules affect nutrient cycling and biomass yields.

2. Model description and testing

2.1. Study area

The study site was in Bantry Bay, a dynamic coastal inlet in south-west Ireland, and included a kelp farm and an adjacent salmon farm (Fig. 1). The kelp farm occupied a licensed area of 60,000 m^2, with 11 lines (each 110 m long) seeded annually with *S. latissima* sporelings in mid-January and harvested between April and June to prevent degradation from epiphyte fouling. The salmon farm, covering 64,000 m^2, comprised three net pens (40 m diameter, 18 m deep), each producing 250 tons of salmon and requiring an equivalent amount of feed. The salmon farm operated from July 2023 to April 2024 after a four-year fallow period, with harvesting beginning in April 2024, during which fish were starved. The two farms were directly adjacent, with the kelp farm located approximately 200 m downstream of the salmon farm.

2.2. Overall modelling approach

The integrated modelling approach (Fig. 2) combines three key components: a salmon growth model, outputs from a hydrodynamic model, and a kelp growth model. Details of the individual model components, the data inputs and testing are given in the following sections, but in brief, the models and outputs are used to simulate and analyse the interactions between the fish farm, local environmental conditions, and kelp growth. The salmon growth model provides daily estimates of dissolved nitrogenous waste that are released into the environment from the salmon farm, based on temperature, feeding and stocking information. Current speed and direction from the hydrodynamic model are then used to simulate transport of the dissolved nitrogenous waste to the kelp farm. The kelp growth model then uses this nitrogenous waste, along with temperature, irradiance and dissolved inorganic carbon (DIC), as inputs to estimate the nitrogen and carbon content and assimilation of kelp over time as well as its growth.

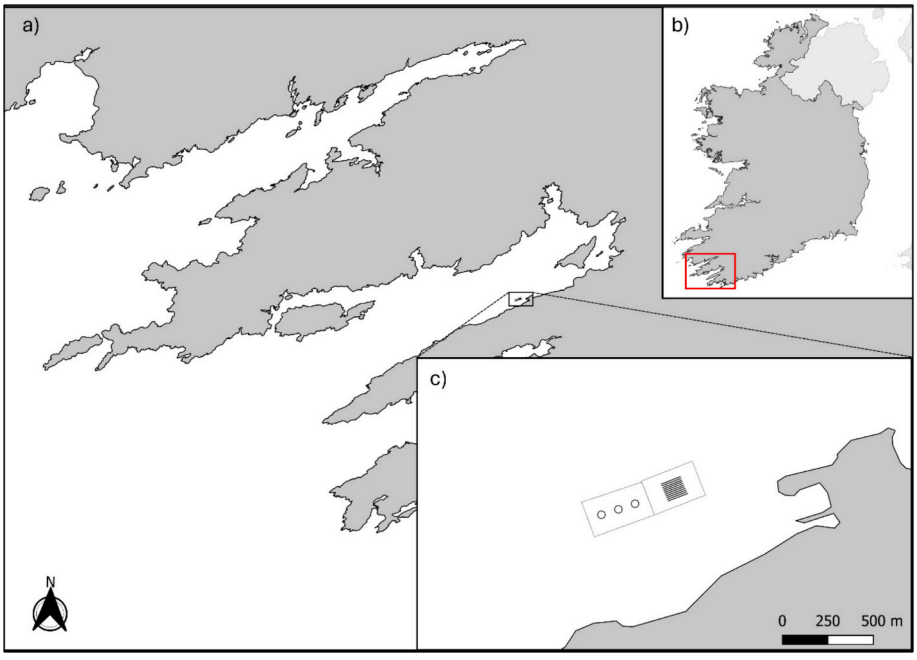

Fig. 1. Study area in a) Bantry Bay, in b) the South-West of Ireland, and c) Study site of an incidental commercial-scale IMTA system, consisting of a 3-net-pen salmon farm and an 11-line kelp farm. The dashed line indicates the licensed area of each farm.

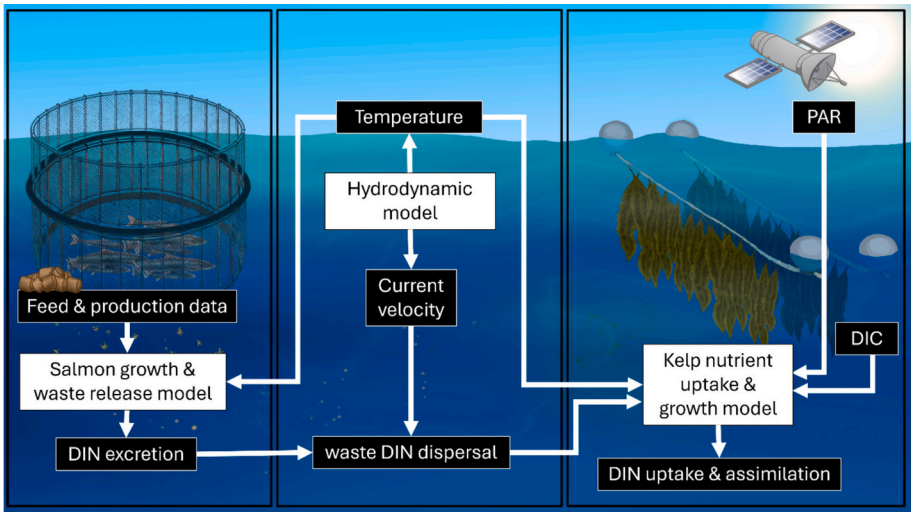

Fig. 2. Illustrative overview of the salmon-kelp IMTA integrated modelling approach developed and used in this study. DIN: dissolved inorganic nitrogen; PAR: photosynthetically active radiation; DIC: dissolved inorganic carbon.

2.3. Simulating the release of dissolved inorganic nitrogen (DIN) by salmon farm

The commercially available model FEEDNETICS version 4.0 [SPAROS, Olhão, Portugal] was used to simulate growth and dissolved inorganic nitrogen (DIN) waste release from the salmon. FEEDNETICS is a dynamic, mechanistic model that simulates fish growth, nutrient utilization, and body composition in aquaculture systems (Soares et al., 2023). The model runs on a daily timestep, offering outputs at this resolution. The model was run for this study site using production data from the salmon farm in Bantry Bay across the 10-month 2023–2024 production cycle. This was an organic production site, certified by the EU Organic Aquaculture Standards (Regulation (EU) 2018/848), Bio Suisse and Naturland, used as a conditioning site for fish stocked at ~1 kg average body weight to market size.

FEEDNETICS required three types of input data: production level, feed characteristics and temperature. The production data for this study is listed in Table 1. Information on feeding strategies, and type and size of feed pellet were obtained from feeding records provided by the salmon producer. Feed data included the proximal composition (Table 2) and amino acid profile (Table 3) of the feed, and these values were sourced from the feed supplier. Only one feed type, typically used at the final stage of production, was assumed to be used throughout the production cycle. This was an organic feed (43.7 % fish meal from trimmings, 17.7 % fish oil from trimmings, 6.3 % vegetable oil). Values for apparent Digestibility Coefficients (ADCs) of crude protein, fat, phosphorus, and gross energy were assumed as 92 %, 98 %, 70 % and 88 % respectively, based on the default values available at FEEDNETICS' for "premium feed". Feed samples (5 replicates) were sent for oil content and fatty acid analysis (methods following Sprague et al., 2020) to obtain the feed fatty acid profile (Table 4). The measured fatty acid profile of the fish feed, expressed as a percentage of total fatty acids, included additional fatty acids not required by the model and lacked two required fatty acids (myristoleic acid and elaidic acid). Their proportions were estimated using FEEDNETICS default values. To ensure the total summed to 100 %, all measured fatty acids were proportionally adjusted while preserving their relative composition. Uneaten feed loss was iteratively adjusted according to the fit of modelled to observed

Table 1
Salmon farm production input data used for testing of FEEDNETICS for the 2023–2024 salmon farm site & production scenario.

Parameter	Value
Species	Atlantic salmon
Start date of production period	05/06/2023
Initial fish weight (g)	1213
Cage volume (m^3)	8423
Production period (months)	10 (305 days)
Initial number of fish	141,675
Monthly mortality rate (%)	4.0

Table 2
Proximate composition of salmon feed used for testing of FEEDNETICS for the 2023–2024 salmon farm site & production scenario.

Nutrient	Amount
Crude protein	38.7 (% WW of feed)
Crude fat	31.4 (% WW of feed)
Ash	8.6 (% WW of feed)
Fibre	1.5 (% WW of feed)
Phosphorous	1.2 (% WW of feed)
Gross energy	13.5 (MJ/kg)

Table 3
Feed fatty acid profile used for testing of FEEDNETICS for the 2023–2024 salmon farm site & production scenario, expressed at percentage of total fatty acids in the feed.

Fatty acid	Composition (% Total Fatty Acids)
Myristic	2.36
Myristoleic	0.11
Palmitic	10.63
Palmitoleic	3.12
Stearic	4.90
Oleic	41.92
Elaidic	3.32
Linoleic	14.28
A-Linoleic	5.53
G-Linoleic	0.07
Stearidonic	0.87
Arachidic	0.53
Eicosenoic	2.65
Eicosadienoic	0.11
Arachidonic	0.28
Eicosapentaenoic	5.20
Erucic	0.42
Docosapentaenoic	0.86
Docosahexaenoic	2.50
Nervonic	0.34

Table 4
Feed amino acid profile used for testing of FEEDNETICS for the 2023–2024 salmon farm site & production scenario, expressed at percentage of total amino acids in the feed.

Amino Acid	Composition (% Total Amino Acids)
Alanine	7.35
Arginine	7.35
Asparagine	5.12
Aspartic acid	5.13
Glutamine	7.84
Glutamic acid	7.84
Glycine	6.56
Histidine	2.68
Isoleucine	4.09
Leucine	7.51
Lysine	7.37
Phenylalanine	4.19
Proline	4.42
Serine	4.69
Threonine	4.48
Tyrosine	3.23
Valine	5.14
Tryptophan (Total)	1.21
Cysteine +Cystine	1.21
Methionine	2.59

growth. Estimated daily temperature data was obtained from the Bantry Bay Regional Ocean Modelling System (ROMS) model (described in section 2.4).

FEEDNETICS produced a time series for average body weight of the fish (g/fish), the number of fish, total fish biomass (kg), and total nitrogenous waste from metabolic processes (kg/day). FEEDNETICS was tested for use at this study site by comparing modelled growth outputs with farm data. Specifically, the final individual fish weight and the total yield obtained from the model was compared with observed values of mean live weight of fish and total yield at harvest, as provided by the fish farm operator. The accuracy of the FEEDNETICS outputs was assessed using the absolute and relative differences between observed and predicted average fish body weight and total biomass at harvest. At the end of the 10-month production period, FEEDNETICS demonstrated an acceptable level of accuracy using a 10 % uneaten feed loss when compared to observed data, although it did overestimate fish average final body weight (Table 5). A 10 % feed loss is acceptable in dynamic sites (Strain and Hargrave, 2005). The modelled hourly release of metabolic N was used as an estimate of continual DIN concentration in the salmon farm environment.

2.4. Modelling nutrient flow from salmon farm to kelp farm

The flow of nutrients from the salmon farm to the kelp farm was estimated based on hydrodynamic data and the nitrogen (N) concentration released by the salmon farm derived from FEEDNETICS. The hydrodynamic data was obtained from an ocean forecasting model of Bantry Bay developed by the Marine Institute (Ireland) using ROMS (Dabrowski et al., 2016). The Bantry Bay ROMS model uses grid cells corresponding to horizontal spacings of 200–250 m and 3 vertical levels (ocean surface, 20 m depth and ocean floor), with time series outputs are generated at 10-min intervals. Time series of surface level current speed, direction, and temperature data between 01/01/2023 and 01/07/2024 were requested from the Marine Institute's data request webpage (https://www.marine.ie/data-request) for the kelp farm location (51°39′10.1"N, 9°34′59.9"W). The modelled time series of surface temperature, current speed and direction were converted to hourly means for further use.

Table 5
Modelled vs observed values for the 2023–2024 salmon farm site & production scenario, using 10 % uneaten feed loss.

	Observed	Modelled	Absolute difference	Relative difference (%)
Average final body weight (kg)	5.57	6.15	0.55	9.87
Total biomass (kg)	523,668	575,958	52,290	9.99
Number of fish	94,101	94,189	88	0.09

Hourly nutrient flow from the salmon farm to the kelp farm was determined as the product of the water volume transported between the salmon and seaweed farms and the N concentration in the water at the salmon farm. The volume of water moving from the salmon farm to the kelp farm is a function of the current speed and the direction of the current relative to the direction between the two farms. The total hourly volume of water moving from the salmon farm towards the kelp farm (Vm) is calculated using Eq. 1.

$$Vm = U \cdot \cos(\theta - \alpha) \cdot As \cdot t \quad (1)$$

Where:

- U is the current speed in meters per second (m.s^{-1}) at the salmon farm, obtained from Bantry Bay ROMS outputs.
- θ is the current direction in degrees, measured clockwise from true north.
- α is the angle between the salmon farm and the kelp farm, measured clockwise from true north. The cosine term $cos(\theta - \alpha)$ adjusts the current speed to reflect only the component that moves towards the kelp farm.
- As is the cross-sectional area in m^2 (determined by the vertical depth and horizontal width of the salmon farm) of the water column at the salmon farm through which water flows.
- t in seconds, which is set to 3600 s (equivalent to one hour, the timestep the kelp model runs on).

The N concentration at the salmon farm was calculated from the total nitrogenous waste from metabolic processes predicted by FEEDNETICS (converted to nitrate using its molar mass) and the volume of the salmon farm. Since this provided the daily mean N concentration, and the kelp model required an hourly input, it was assumed that 70 % of the N waste is released within two hours of feeding at 8.00 a.m., based on post-prandial N release from salmon as reported by Reynolds (2005). Therefore, the model assumed that 35 % of the daily N waste was released at 9.00 a.m. and another 35 % at 10.00 a.m.. The remainder of the waste was divided into the other 23 h. The 3-month-mean background N concentration, as measured from the kelp farm in absence of salmon farming, was added to all hourly N inputs to the kelp farm (see Supplementary Material Section A, for nutrient sampling details).

Thus, the total amount of nitrate transported per day (N_{moved}) was calculated using Eq. 2.

$$N_{moved} = V_m \bullet N_{conc} \quad (2)$$

Where:

- N_{moved} is the total mass of nitrate transported from the salmon farm to the kelp farm (kg.hr^{-1}).
- N_{conc} is the nitrate concentration at the salmon farm in kg.m^{-3}.hr^{-1}, as calculated by FEEDNETICS metabolic N output (kg N day^{-1}), the volume of the salmon farm, and modified to an hourly timestep according to post-prandial N release by salmon.
- V_m is the volume of water moving from the salmon farm to the kelp farm (m^3.hr^{-1})' as calculated in eq. 1.

And the hourly concentration of N at the kelp farm (N_{kelp}) in kg.m^{-3}.hr^{-1} is calculated using Eq. 3.

$$N_{kelp} = \left(N_{moved} / V_{kelp}\right) + N_{background} \quad (3)$$

Where:

- V_{kelp} is the volume of the kelp farm (m^3), calculated from the farm surface area (m^2) and culture depth (1 m).
- N_{moved} is the total mass of N transported from the salmon farm to the kelp farm ($kg.hr^{-1}$)
- $N_{background}$is the background N concentration at the kelp farm ($kg.m^{-3}.hr^{-1}$), as calculated from N measurements at the kelp farm when no salmon farming is present.

Assumptions used in these calculations are, firstly, that N is evenly distributed within the water column to the depth of the salmon farm, so the total N transported depends on both the volume of water that from the fish farm which passes through the kelp farm and the N concentration within that volume. Secondly, that waste at kelp farm is not cumulative with each hourly time-step, and the waste entering would leave within the hour.

The modelled N_{kelp} was compared to in situ total nitrogen (TN) concentration measurements taken from the kelp farm in 2024, during the same time when the salmon farm was active (Fig. 3). Absolute error and percentage error were calculated by comparing the modelled N_{kelp} to the mean of the observed total nitrogen (TN) concentrations, based on 10 water samples collected per month. The modelled vs observed results indicate that while the calculated N_{kelp} shows a reasonable alignment with the observed data, the high relative difference values during spring (Mar-April) are indicative of the large range of TN in observed data (Table 6). An overall root mean squared error (RMSE) and mean average percentage error (MAPE) was calculated as 0.08 $mg.L^{-1}$ TN and 44.03 % respectively. The large April MAPE (>75 %) arises primarily from comparing a relatively small absolute difference (0.070 $mg\ L^{-1}$) to a low observed mean (0.093 $mg\ L^{-1}$), which inflates percentage error at low concentrations.

2.5. Kelp nutrient uptake & growth: the kelp DEB model and re-parameterisation

Kelp nutrient uptake, assimilation and growth was simulated using a re-parameterisation of a DEB model developed for kelp by Venolia et al. (2020), hereafter referred to as the Kelp DEB. The model was implemented in R version 4.4.1 (R Core Team, 2024), using the packages deSolve (Soetaert et al., 2008) and pracma (Borchers, 2011).

2.5.1. Kelp DEB structure

The Kelp DEB model tracks the uptake of carbon and nitrogen, their assimilation into reserves, and their allocation towards growth, maintenance, or excretion. State variables included the structural volume of a kelp plant (M_V in mol V, moles of structure), its nitrogen reserve density (m_{E_N}, in mols N/mol V), and carbon reserve density (m_{E_C}, in mol C/mol V). The outputs for the Kelp DEB model included the moles of each state variables, as well as rates and flows associated with N and C assimilation and utilization (either for maintenance, for growth, or rejected and then either returned to the reserves or excreted). The dry weight of a single kelp plant (DW) in grams was derived by converting M_V, m_{E_N} and m_{E_C} to mass using their respective molar masses (w_{E_N}, w_{E_C}) and adding them together. Additionally, the percentage of the DW that consists of carbon and nitrogen was calculated by quantifying the mass of each reserve (molar mass of reserve i * m_{E_i} * M_V), plus the proportion of M_V that is N and C (based on the stoichiometric composition of M_V) (See Table 7). The Kelp DEB model estimated kelp blade length via an empirical relationship with DW. The Kelp DEB model runs on an hourly timestep, and all rates were temperature corrected, based on the Arrhenius equation. For more details of the model structure, mathematical equations and constants, refer to tables S1 and S2 in the Supplementary Material Section B and Venolia et al. (2020).

The kelp DEB required time series of temperature, DIN, DIC and irradiance. Temperature was obtained from the Bantry Bay ROMS model, and DIN was derived from FEEDNETICS and subsequent hydrodynamic transport (Section 2.4). DIC forcings were assumed to be constant, and previously reported values of 2083 µM DIC for Bantry Bay were used (McGrath et al., 2019). Irradiance forcing was derived from satellite data, specifically photosynthetically active radiation (PAR) measurements from the NOAA-20 VIIRS (NASA Ocean Biology Processing Group, 2022), with a daily and 4 km spatial resolution. Subsurface PAR was computed with the Beer–Lambert law, $PAR(z) = PAR_0 e^{K_d z}$, assuming a fixed diffuse attenuation coefficient, K_d, of 0.1 m^{-1}, representative of the lower-bound of K_d in NE Atlantic coastal waters (McKee et al., 2007; Son and Wang, 2015). Site water samples and sediment-trap observations indicated consistently low SPM during the study period. After accounting for light attenuation at 1 m depth, satellite PAR was calculated in mol photon.m^2.h^{-1} and this was applied over the day as a 12:12 photoperiod, with no light from 20.00 p.m. to 08.00 a.m..

2.5.2. Re-parametrisation of site-specific values

The kelp DEB model was re-parametrised so that modelled kelp growth outputs fitted farmed kelp growth data from 2024 (production period 16 January to 14 April; see Supplementary Material Section A for sampling information), a year when the kelp were exposed to elevated nitrate from nearby salmon farming. Re-parametrisation involved iterative adjustments to model parameters to align predictions with observed kelp blade length, blade dry weight and tissue composition metrics (C content (% DW), N content (% DW). Specific parameters optimized were stoichiometric composition of the different state variables (M_V, m_{eN} and m_{eC}, which were composed of alginate, nitrite/

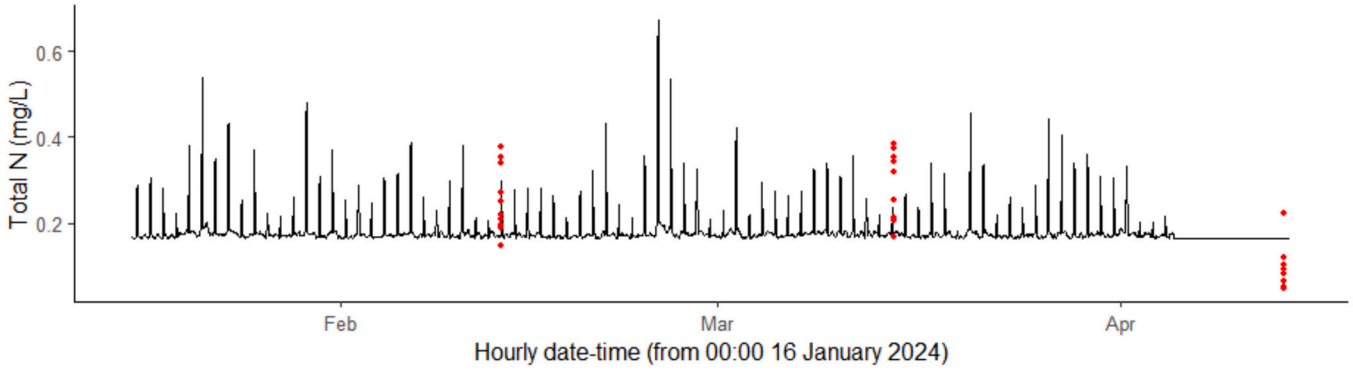

Fig. 3. Total N modelled at the kelp farm (black line), derived from: FEEDNETICS output of Total Metabolic N (kg/day) for the salmon production period overlapping with kelp production, converted to hourly outputs according to the ratio of 70 % of waste being released within 2 h post-feeding, and then modified to N transported to kelp farm using Bantry Bay ROMS hydrodynamic forcing. Red points overlaid to show in situ TN measurements taken during the kelp production period. (For interpretation of the references to colour in this figure legend, the reader is referred to the web version of this article.)

Table 6
Modelled vs observed values for N_{kelp} calculated from model simulations and in situ TN measurements taken at the kelp farm at 3 different times during the 2023/2024 salmon production season ($n = 10$).

Date-Time	Average observed TN ± SD (mg. L^{-1})	Range of observed TN (mg. L^{-1})	Modelled TN (mg. L^{-1})	Absolute difference (TN mg. L^{-1})	Relative difference (%)
13 Feb 2024, 10:00	0.255 ± 0.078	0.147 to 0.377	0.292	0.037	14.51
15 Mar 2024, 10:00	0.282 ± 0.081	0.166 to 0.385	0.169	0.113	40.07
14 Apr 2024, 10:00	0.093 ± 0.051	0.046 to 0.223	0.163	0.070	75.27

Table 7
Equations for Kelp DEB derived from this study.

Equation	Description
$\%C_{DW} = \frac{M_V\left(m_{E_C}w_{E_C} + \frac{0.04}{3.37}w_V\right)}{DW}$	Percentage of DW carbon
$\%N_{DW} = \frac{M_V\left(m_{E_N}w_{E_N} + \frac{1}{3.37}w_V\right)}{DW}$	Percentage of DW nitrogen
Needed site-specific re-parameterisation (see Section 2.5.2)	Blade length to DW relationship

nitrate, and glucose, respectively, in Venolia et al. (2020), and whose molar weights are given by W_V, W_{EC}, and W_{EN} respectively), and C & N half-saturation uptake coefficients (K_C and K_N respectively) to better match the nutrient concentrations of this site.

The final parameters (K_N, K_C, W_V, W_{EC}, W_{EN}) resulting from the iterative re-parametrisation process are given in Table 8. The original K_C and W_V was deemed to give the best fit to observed data, however K_N was increased from $2.5e^{-6}$ mol NO_3^- L^{-1} to $4e^{-6}$ mol NO_3^- L^{-1}, more similar to Broch and Slagstad (2012); the molar weight of mannitol was used as W_{EC} as it is the major carbohydrate storage compound in *S. latissima* (Stévant et al., 2017) and nitrate was used as W_{EN} as it is stored in vacuoles in kelp tissue for later use (Lubsch and Timmermans, 2019; Ding et al., 2025b).

To assess model robustness to parameter uncertainty, a Monte Carlo correlation-based sensitivity analysis was conducted following established protocols (Hamby, 1994; Saltelli, 2008). The re-parameterised parameters were independently sampled from uniform distributions across biologically realistic ranges: K_N ($0.1e^{-6}$ to $5.0e^{-6}$ mol NO_3^- L^{-1}), K_C ($1e^{-7}$ to $1.01e^{-6}$ mol DIC. L^{-1}), W_{EC} (25 to 35 g.mol^{-1}), W_{EN} (55 to 65 g.mol^{-1}), and W_V (30 to 40 g.mol^{-1}). One hundred Monte Carlo simulations were performed with identical initial conditions and forcing functions in R version [4.4.1.] (R Core Team, 2024), with a fixed random seed for reproducibility. Parameter sensitivity was quantified using Pearson correlation coefficients between the input parameters (K_N, K_C, W_{EC}, W_{EN}, and W_V) and five output variables (final biomass, final length, mean growth rate, final nitrogen content, final carbon content). The sensitivity analysis showed K_N to be the dominant driver of final dry weight ($R^2 = -1.00$), length ($R^2 = -1.00$), and tissue N content ($R^2 = -0.92$), while W_V drove tissue C content ($R^2 = 0.95$) (Fig. S2, Supplementary Material Section C). Despite the strong correlation between these variables, absolute changes in DW and length were minimal. However, variation in K_N and W_V led to more substantial changes in tissue N and content respectively.

Additionally, the relationship between blade length (L) and dry weight (DW) was specifically calibrated for farmed kelp grown at this site, using 2023 and 2024 measured blade length (cm) & DW (g) data accurately capture site-specific growth dynamics. Since the fitted relationships were similar across years, both datasets were combined to improve robustness and applicability across modelled scenarios. A power function of the form $L = c \bullet DW^d$ was fitted to the data. To linearize the relationship, both variables were natural log-transformed, yielding the linear model $ln(L) = ln(c) + d \bullet ln(DW)$. Parameters $ln(c)$ and d were estimated via ordinary least squares regression. The coefficient c was obtained by exponentiating the intercept term. Model fit was assessed using the coefficient of determination (R^2) on the log-log scale. A 95 % confidence interval for the predicted length values was calculated on the log-transformed scale and back-transformed to the original scale for visualization. All analyses and plotting were conducted in R version [4.4.1.] (R Core Team, 2024). The regression model established a site-specific relationship between L and DW for farmed kelp in Bantry Bay, described by the equation: $L = 65.0119 \bullet DW^{0.45}$(Fig. 4). This model exhibited a strong fit to the observed data, with an $R^2 = 0.8815$, but it was noted that it may overestimate L for DW values greater than 1 g.

After applying the 2024 recalibrated parameters and site-specific L-DW relationship to the fully integrated modelling approach and comparing to 2024 observed growth and composition, the results demonstrated good model fit to observed values. Blade DW predictions yielded an RMSE of 0.03 g and a MAPE of 6.37 % (Fig. 5a), while blade length predictions achieved an RMSE of 6.25 cm and a MAPE of 17.70 % (Fig. 5b). Predictions for nitrogen content exhibited an RMSE of 0.07 % DW and a MAPE of 1.88 % (Fig. 5c), while carbon content predictions showed an RMSE of 6.00 % DW and a MAPE of 21.61 % (Fig. 5d). When fitting modelled outputs to exponential growth curves for L and WW fitted from measured data (see Supplementary Material A for measurement details), the model appears to track the general WW growth trend of the empirical data reasonably well (RMSE: 1.15 g, MAPE: 11.76 %), and accurately shows the exponential increase in wet weight over time – albeit overestimating WW in the later part of the growing season (Fig. 6a). In terms of L, the model overestimates blade length in the early

Table 8
Kelp DEB model parameters from Venolia et al. (2020), re-parametrised for application to *S. latissima* grown in Bantry Bay.

Parameter	Parameter description	Parameter Units	Original value (Venolia et al., 2020)	Original environmental conditions (Venolia et al., 2020)	*Re*-parameterised value	This study's environmental conditions
K_N	Half-saturation concentration for NO_3^- uptake	mol NO_3^- L^{-1}	$2.5 * 10^{-6}$	2.5 to 88 μM NO_3^- (laboratory)	$1.5 * 10^{-6}$	2.4 to 19.35 μM NO_3^- (modelled)
K_C	Half-saturation concentration for CO_2 uptake	mol CO_2 L^{-1}	$4 * 10^{-7}$	1835 μM DIC	$4 * 10^{-7}$	2083 μM DIC
w_V	Molar weight of structure	g mol V $^{-1}$	29.89 (Alginate + structural N)	n/a	29.89 (Alginate + structural N)	n/a
w_{EC}	Molar weight of C reserve	g C mol C^{-1}	30 (Glucose)	n/a	30.33 (Mannitol)	n/a
w_{EN}	Molar weight of N reserve	g N mol N^{-1}	54 (Nitrate & Nitrite)	n/a	62 (Nitrate only)	n/a

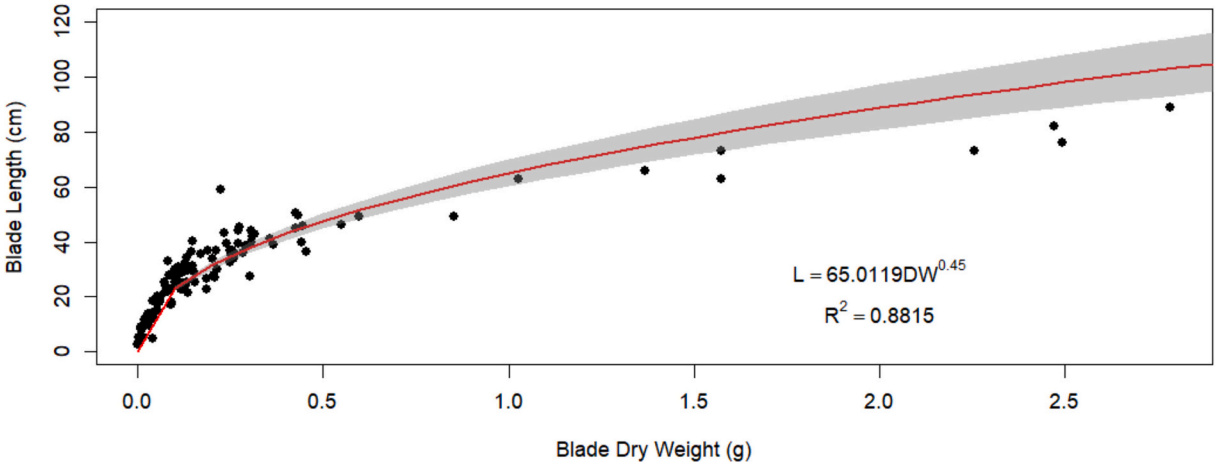

Fig. 4. Power function regression of blade dry weight (DW; g) and blade length (L; cm) for *Saccharina latissima* blades collected from Bantry Bay in 2023 and 2024. The relationship was modelled using a power function of the form $L = c \bullet DW^d$, where parameters were estimated by linear regression following natural log-transformation of both variables. The red line represents the back-transformed fitted relationship on the original scale. The shaded grey area denotes the 95 % confidence interval for the predicted values, derived from the log-transformed model and back-transformed to the original scale. (For interpretation of the references to colour in this figure legend, the reader is referred to the web version of this article.)

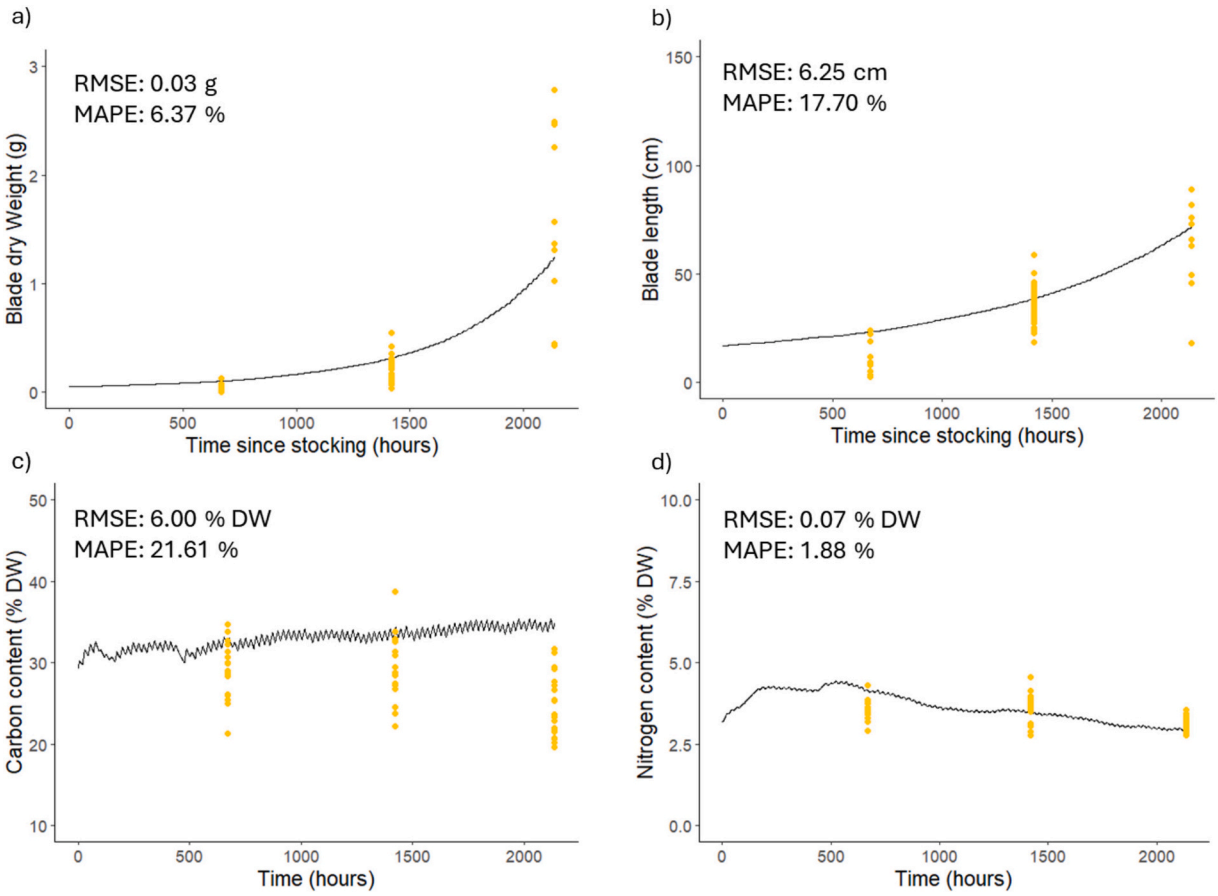

Fig. 5. Results of integrated model validation with 2024 kelp growth data (using 2024 parameters shown in Table X), showing modelled values (black line) vs measured values (yellow points). At each time point, $n = 25$ for blade length and DW observations; $n = 20$ for C & N content. (For interpretation of the references to colour in this figure legend, the reader is referred to the web version of this article.)

part of the growing season (February and March) and underestimates it in the later stages (April and beyond) (Fig. 6b) and thus shows a moderate error (RMSE: 10.61 cm, MAPE: 38.16 %).

3. Model IMTA production scenario development and application

Following re-parameterisation, several production scenarios were applied (Table 9). This included the baseline 2023–2024 production

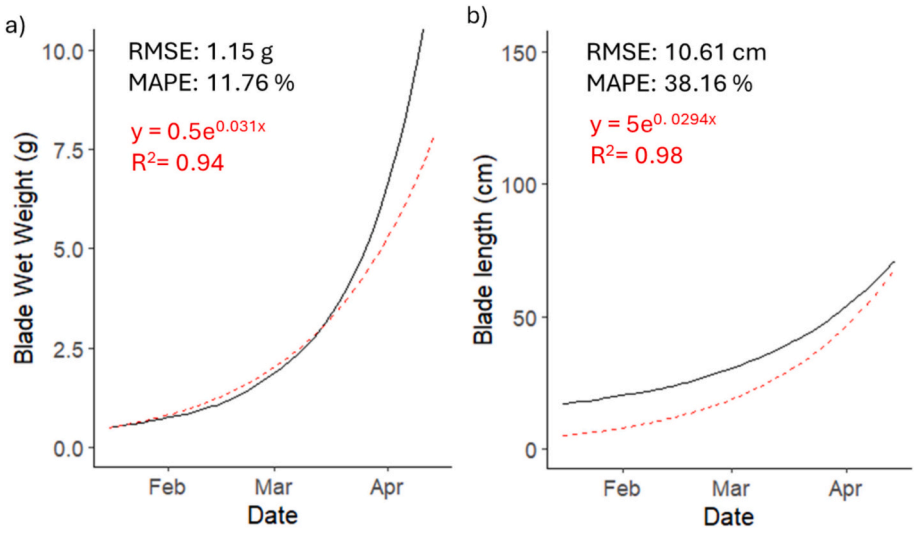

Fig. 6. Results of integrated model validation with empirical exponential growth curves created from 2024 kelp growth data. Modelled values shown as black solid lines vs empirical exponential growth curves as red dashed lines. Equation of empirical growth curves indicated in red. RMSE and MAPE between empirical growth curved and modelled growth shown on figure. (For interpretation of the references to colour in this figure legend, the reader is referred to the web version of this article.)

Table 9
Production scenarios for the salmon-kelp IMTA to be applied to the integrated modelling approach. Baseline scenario corresponds to reported production practice at this site over 2023–2024.

Scenario name	Salmon production	Kelp production
1. Baseline (summer salmon & winter kelp stocking)	5 June– 4 April ~171 t stocking	16 January – 14 April
2. Increased salmon production	5 June– 4 April ~ 483 t stocking	16 January – 14 April
3. Change in timing of kelp farming (late-autumn stocking)	5 June– 4 April ~171 t stocking	1 November – 31 March
4. Change in timing of salmon farming (autumn stocking)	1 October– Aug ~171 t stocking	16 January – 14 April

scenario (summer salmon stocking and winter kelp stocking), and several hypothetical scenarios to simulate the effect on kelp growth and nutrient uptake due to: increased salmon production, a change in the timing of salmon production (autumn stocking), and a change in the timing of kelp farming (late autumn stocking). Since the kelp DEB model gives a DW output for an individual plant, it was necessary to scale up the results to estimate total biomass yield at the kelp farm. Modelled DW values of individual plants were converted to wet weight (WW) by multiplying by 10, according to standard practice. To calculate the total biomass of kelp at farm level, the plant density (kelp plants per meter) of the farm, and the length (m) of rope seeded with kelp in the farm is required. Based on current production practices, the average *S. latissima* yield at this farm is historically 6 kg WW/m. From measured growth data, the average final WW of an individual plant in 2024 and 2023 was 0.0094 kg. Using these values, the estimated plant density is 638 plants per meter. To calculate total kelp biomass, the final model output for individual plant weight (kg WW per plant) is multiplied by 638 plants per square meter and then by the total farm rope length of 1100 m, yielding the final biomass estimate. This can be summarised in Eq. 4:

$$Total\ kelp\ biomass = DW \bullet 10 \bullet \rho_{kelp} \bullet x, \quad (4)$$

Where:

- DW is the modelled dry weight of an individual kelp plant in kg.
- ρ_{kelp} is the plant density of the kelp farm in plants per m.
- x is the length of seeded rope in the kelp farm in m.

To assess the scalability of kelp-based bioremediation, the number of kelp lines required to mitigate 10 % of salmon metabolic nitrogen waste was estimated for each scenario. The area required for these lines was mapped and positioned to the north and northeast of the salmon farm, aligning with prevailing current directions to maximize interception of waste-derived nutrients. The mapping assumed a 10 m spacing between kelp lines.

4. Results

The IMTA model outputs (Table 10) show that among the four scenarios, only changing kelp stocking timing and lengthening the production period (Scenario 3; 151 days) produced changes in modelled kelp yield and nitrogen assimilation that exceed 1 percentage point; Scenarios 1 (Baseline), 2 (increased salmon production), and 4 (autumn salmon stocking) differ in assimilation by <1 percentage point with kelp yield remaining ~8.71–8.72 t per farm. Increasing salmon production in Scenario 2, which nearly tripled the nitrogen waste from salmon farms, did not result in increased kelp growth or nitrogen assimilation compared to the Baseline. Similarly, changing the timing of salmon production to overlap more with kelp farming in Scenario 4 marginally improved nitrogen assimilation to from 0.71 to 0.84 % and kelp yield remained consistent with the Baseline.

In contrast, extending the kelp growing season (late-autumn stocking) in Scenario 3 had a marked impact on kelp growth performance. The model outputs of kelp yield suggests that by extending the production period, the kelp would achieve a peak growth rate and substantially greater biomass yield, reaching approximately 32.71 t per farm. This extended cycle predicts a larger blade size, exceeding 100 cm length, compared to the ~65 cm limit observed in the shorter production cycles, indicating both larger plants and a greater absorption area. The growth rate of kelp in Scenario 3 was predicted to be slower over the first three months (0.53 g DW, 50 cm blade length) compared to the other scenarios (1 g DW, 63 cm blade length) (Fig. 7a, b). However, the average net specific growth rate over the entire production season was 4.58 mol.h^{-1} for Scenario 3, considerably higher than the 2.01 mol.h^{-1} for Scenarios 1, 2, and 4.

Model outputs of kelp blade dry weight indicate that a longer culture period would allow the kelp to reach peak biomass, unlike the shorter

Table 10
Modelled outputs of IMTA integrated modelling approach for 4 different production scenarios.

Scenario	Total salmon yield (t)	Total salmon metabolic N waste (t)	Kelp production period (days)	Total kelp yield per farm (t)	Net N assimilation per farm (kg)	N assimilation (% N metabolic waste)	Number of 110 m kelp lines to remediate 10 % of salmon waste (yield and area)
1. Baseline (summer salmon & winter kelp stocking)	575.96	15.35	89	8. 71	109.43	0.71	155 lines (123 t WW kelp yield; 34.70 ha)
2. Increased salmon production	1373.01	40.45	89	8.72	110.97	0.27	401 lines (318 t WW kelp yield; 83.95 ha)
3. Change in timing of kelp farming (late-autumn stocking and double production time)	575.96	15.35	151	32.71	471.44	3.07	36 lines (107 t WW kelp yield; 6.14 ha)
4. Change in timing of salmon farming (autumn stocking)	536.59	13.10	89	8.71	109.70	0.84	132 lines (105 t WW kelp yield; 27.93 ha)

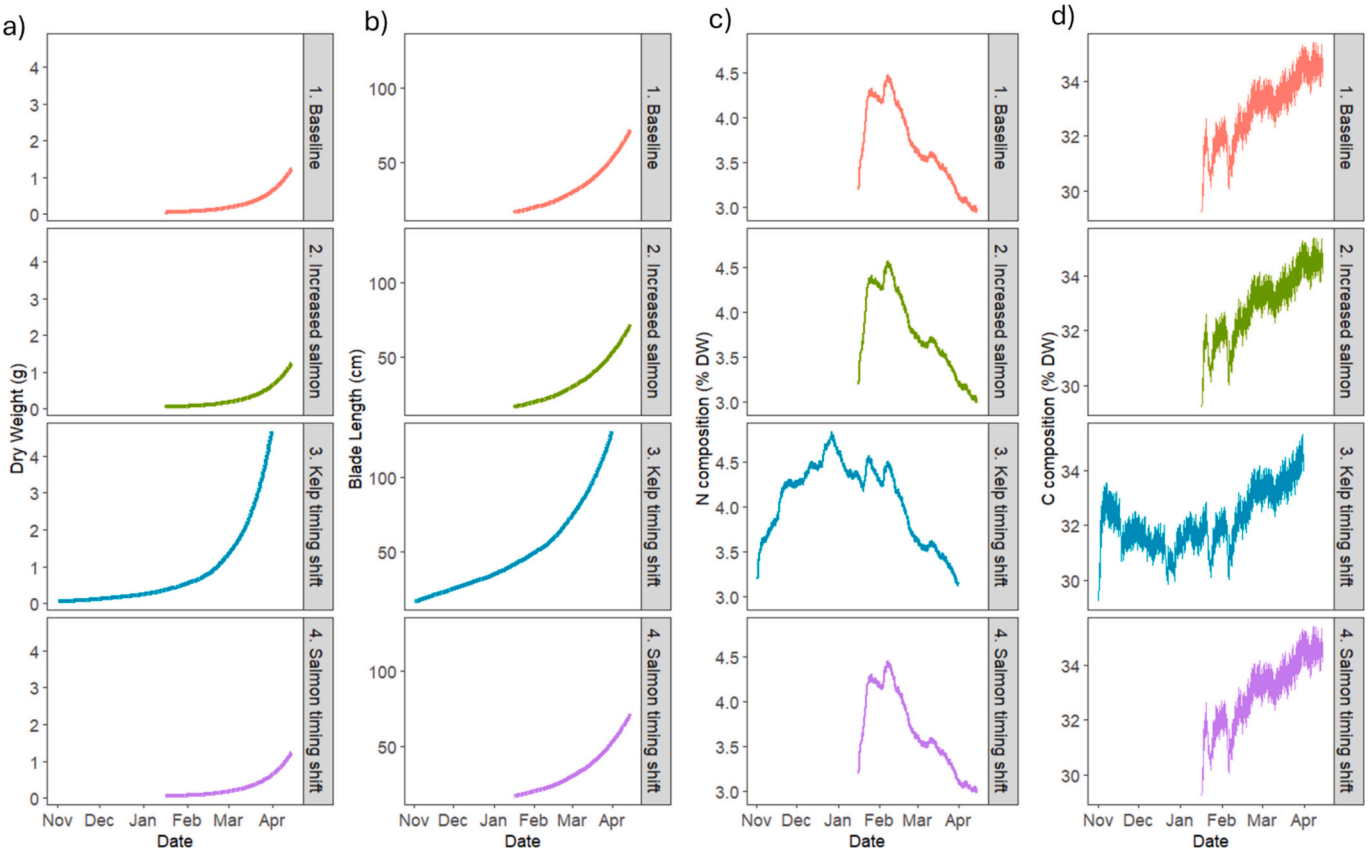

Fig. 7. Kelp DEB output for 4 different salmon-kelp production scenarios of the IMTA system in Bantry Bay: individual kelp plant a) dry weight (g), b) kelp blade length (cm), c) kelp blade N composition (%DW), and d) kelp blade C composition (%DW).

production cycles where kelp would be harvested before reaching its full potential (Fig. 7a). In Scenario 3, the modelled kelp has a strong exponential growth pattern, with the growth rate accelerating considerably towards the end of the extended production period, reaching its maximum growth rate in March or April. In contrast, the growth curves for the other scenarios are shallower and remain almost linear throughout the shorter production cycles, indicating slower and more consistent growth. These scenarios do not allow the kelp to reach its exponential growth phase or maximum growth rate, as harvest occurs before this phase is realized. Model outputs of tissue N and C content suggest that there would not be marked differences in nitrogen and carbon composition at the end of the production cycle between scenarios (Fig. 7c, d), implying that the effect of environmental N on these variables is saturated, and they are influenced by other environmental forcings. This was noticeable in the kelp DEB output where a greater proportion of N was rejected from growth during the early growth season (November – January), corresponding to light-limited periods (Fig. S3, Supplementary Material Section D).

From a bioremediation perspective, the modelled scenarios suggest that extending the kelp growing season (Scenario 3) would remove 471.44 kg (3.07 %) of salmon metabolic nitrogen waste, a four-fold increase from the baseline scenario which suggests removal of 109.43 kg (0.71 %) of nitrogen (Table 10). Notably, model N assimilation outputs also suggest that increasing salmon production (Scenario 2) would

not improve bioremediation performance, re-iterating that the kelp farm is not nitrogen-limited and that excess nitrogen from salmon farming would not enhance kelp's capacity to absorb waste. N assimilation outputs also suggest that stocking salmon in October rather than June (Scenario 4), would have a negligible increase in nitrogen assimilation, at 109.70 kg (0.84 %) compared to the baseline (Table 10).

The number of kelp lines required to bioremediate 10 % of salmon metabolic nitrogen waste varied across scenarios (Table 10). In the baseline scenario (Scenario 1), the results suggest that 155 kelp lines would be required. Changing the salmon stocking date to October rather than June (Scenario 4) would reduce this to 132 lines. However, stocking the kelp earlier and extending the growing season (Scenario 3) would require only 36 lines (the fewest of all scenarios examined) while still fitting within the currently licensed kelp farm area. In contrast, increasing the number of salmon (Scenario 2) would require the most extensive deployment, at 401 kelp lines. The potential spatial extent of kelp required under each scenario is shown in Fig. 8.

5. Discussion

The aim of this study was to examine the effect of different salmon-kelp stocking strategies on kelp growth and bioremediation in a coastal salmon-kelp IMTA system. To do this, an integrated modelling approach was developed that allowed the simulation of a salmon-kelp IMTA system in Bantry Bay, Ireland. The integrated modelling approach combined a nutrient-based salmon growth model (FEEDNETICS), hydrodynamic simulations (Bantry Bay ROMS), and a re-parameterised kelp DEB model. Applying this modelling framework to a commercial-scale IMTA system allowed for the validation of the model in a real-world aquaculture setting. Such applications are necessary for validating theoretical models and improving their relevance to operational settings, particularly as interest in scaling up IMTA systems continues to

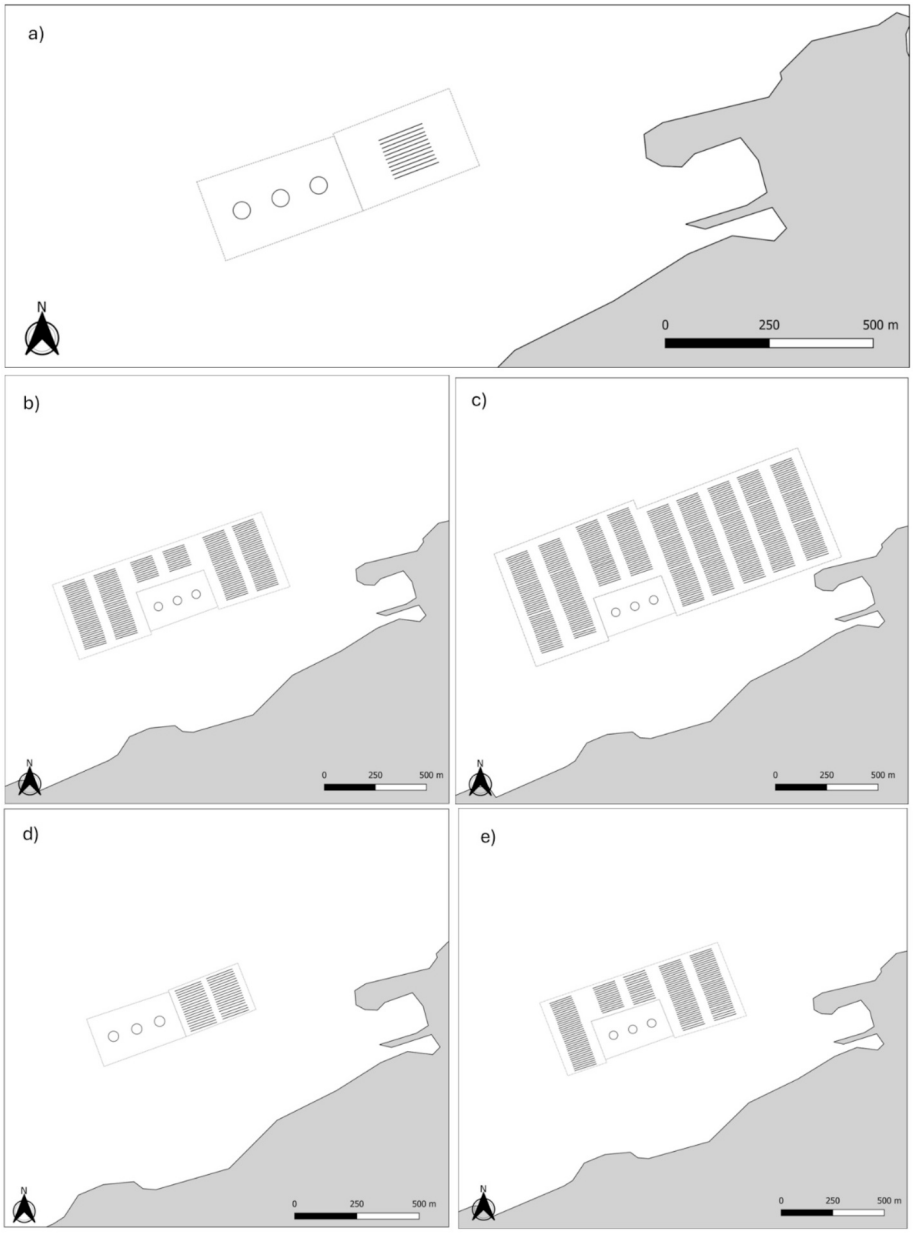

Fig. 8. The potential spatial extent of kelp lines required to bioremediate 10 % of salmon metabolic nitrogen waste under each scenario. Panel (a) shows the baseline salmon farm layout without additional kelp lines. Panels (b)–(e) show the estimated number and placement of kelp lines for Scenario 1 (baseline conditions, 155 lines), Scenario 2 (increased salmon biomass, 401 lines), Scenario 3 (earlier kelp stocking and extended growing season, 36 lines), and Scenario 4 (later salmon stocking, 132 lines), respectively. The dashed line indicates the area of each farm.

grow. Overall, the integrated modelling approach demonstrated acceptable accuracy in predicting overall salmon growth and general trends in kelp biomass and was useful for comparing different IMTA stocking scenarios.

5.1. Kelp growth performance in IMTA production scenarios

There were negligible differences in modelled kelp growth across Scenarios 1, 2, and 4, despite Scenario 2 releasing 3 times more metabolic N waste than Scenario 1 or 4. This suggests that nitrogen availability would not be the primary limiting factor for kelp growth at this site, as increased nitrogen availability did not lead to increased uptake or growth of the modelled kelp. This finding aligns with studies indicating that kelp growth can be constrained by other environmental factors, such as light availability, temperature, and hydrodynamics (Gerard, 1987; Broch and Slagstad, 2012; Hadley et al., 2015; Bruhn et al., 2016). Furthermore, research suggests that *S. latissima* exhibits nitrogen uptake saturation at nitrate concentrations of approximately 10 μM (0.62 $mg.L^{-1}$), beyond which additional nitrogen does not significantly enhance growth (Wang et al., 2022). The modelled nitrate levels in this study regularly surpassed 0.62 $mg.L^{-1}$, particularly at times of postprandial pulse excretion by the salmon. Hence, at this location, it is likely that increased nitrogen forcing or changes in salmon production timing would not have a noticeable effect on kelp production since the farmed kelp would be near its nitrogen uptake limit (Lubsch and Timmermans, 2019). The re-parametrisation of K_N to a higher value implies that kelp here have a lower affinity for nitrate than those studied in the original model (Venolia et al., 2020). This finding is consistent with acclimation of kelp to a high N environmental, reducing uptake levels (Roleda and Hurd, 2019; Forbord et al., 2021). Given that the kelp DEB in this study was forced with nitrate of 11.6 to 84.1 μM, the uptake fraction $\frac{S}{K_N+S}$ lay between 0.74 and 0.96. Uptake is therefore high across most of the production period, but not saturated, indicating that kelp were rarely nitrate-limited, yet growth remained sensitive to K_N relative to the other varied parameters (as confirmed by the sensitivity analysis). Therefore, optimisation of the salmon-kelp IMTA at this site would largely depend on the kelp stocking strategy rather than the salmon.

Model outputs indicated reduced growth rates for kelp deployed in November (Scenario 3) compared to deployments in January (Scenarios 1, 2, and 4), coinciding with periods of lower irradiance. This pattern aligns with previous research demonstrating that light availability is a key determinant of *S. latissima* growth (Bruhn et al., 2016; Azevedo et al., 2019), and that seasonal fluctuations and turbidity from resuspension can substantially limit light penetration at cultivation depth (implying a dynamic K_d, relating to seasonal turbidity should be implemented in future model use). The slower initial growth observed in Scenario 4 is consistent with the documented effects of reduced daylight during late autumn and winter on kelp productivity (Sharma et al., 2018). This interpretation is further supported by the elevated values of $J_{E_N}R$ (the flux of nitrogen in the reserve rejected from growth) during winter months (Fig. S3, Supplementary Material Section D), indicating that nitrogen availability exceeded the energy required for assimilation, due to light limitation.

It should be noted that the kelp DEB model currently does not account for self-shading effects and nutrient competition, both of which can influence kelp growth, especially in high-density systems (Roleda and Hurd, 2019). Incorporating these dynamics into the model could improve predictions, especially in scenarios with high kelp densities. Additionally, incorporating frond erosion processes would improve biomass estimates in high-energy environments (Fieler et al., 2021; Ding et al., 2025a).

Nevertheless, the results also indicate that there might be benefits at this site if kelp was deployed in November and the growing season was extended, as in Scenario 4 the modelled kelp reached its exponential growth phase and achieved greater biomass. Despite initially reduced growth due to lower light levels, extended cultivation resulted in approximately four times the biomass accumulation compared to the other scenarios. By the time optimal light and temperature conditions arrived in March–April, kelp in Scenario 3 had already developed a substantial biomass, allowing for increased nitrogen uptake due to a larger surface area available for absorption. This dynamic suggests that early deployment could enhance nitrogen removal later in the season.

However, an extended deployment must also be viewed in the context of logistical and environmental constraints. While longer cycles clearly enable peak growth, they may also expose kelp farms to greater risks, including fouling and storm damage (Bannister et al., 2019; Veenhof et al., 2024). The trade-off between maximizing yield and minimizing risk presents a challenge for kelp producers. A shorter production cycle timed to coincide with late winter and spring, when daylight and environmental conditions are more favourable, could offer a compromise, also potentially minimizing production costs (Coleman et al., 2022).

5.2. Bioremediation performance in IMTA production scenarios

The modelled bioremediation potential of kelp ranged between 0.27 % and 3.07 % of the total N released from the salmon waste, with the extended kelp growing season (Scenario 3), removing the largest amount of N. This is within the broad range of N assimilation figures from other open-water studies in the North Atlantic: 0.41 % (Broch et al., 2013) to 12 % (Fossberg et al., 2018) dissolved nitrogen removal. However, there is currently no agreed threshold for what constitutes ecologically or operationally meaningful nitrogen removal in this context. As such, these findings underscore ongoing uncertainty around how much removal is required to produce a measurable environmental benefit, and whether the scale of cultivation required is practical in real-world farming systems (Broch et al., 2013; Fossberg et al., 2018; Chary et al., 2020; Christensen, 2020). Rather than implying sufficiency, these modelled values should be interpreted as an indication of the relative potential under different farming scenarios, and a prompt for further work on nutrient transport, ecosystem response, and bioremediation efficacy.

Considering scale-up, achieving a 10 % reduction in salmon-derived nitrogen waste would require extensive kelp infrastructure across most scenarios. Scenario 3, which performed best in terms of bioremediation, would require a kelp farm expansion from 11 to 36 lines of 110 m each to achieve 10 % nitrogen assimilation. This is a substantial but potentially feasible expansion, as it would fit within the current licensed area of the kelp farm of ~6 ha. An even greater expansion is needed in the baseline scenario, which would require 155 lines (approx. 35 ha) or the increased salmon production scenario, which would require 401 lines (approx. 84 ha).

To put this into perspective, total cultivated kelp production in Ireland in 2019 was 42 t live weight (Bord Iascaigh Mhara, 2023). In contrast, achieving 10 % nitrogen bioremediation at this single site would require an estimated kelp biomass yield of 123 t (Scenario 1), 318 t (Scenario 2), 105 t (Scenario 3), or 107 t (Scenario 4). Even the most efficient scenario would require a ~ 70 % increase in production volume of the country's total farmed output that year. These results suggest that scaling kelp production to support nutrient mitigation services would require not only spatial expansion but also substantial increases in national production capacity, along with associated harvesting, processing, and market capacity. Existing post-harvest infrastructure represents a major bottleneck to scale-up (Stévant and Rebours, 2021; Koch et al., 2024; Cerca et al., 2024). For example, the drying capacity required to handle large increases in harvested kelp may not currently be available or economically viable. Therefore, while Scenario 3 demonstrates biological potential for enhanced kelp-based bioremediation, its practical feasibility will ultimately depend on addressing these broader logistical and operational challenges.

The scale of expansion required for bioremediation also raises

important spatial management questions about licensing and operational feasibility (e.g. space for well-boat navigation), but also about optimal placement of kelp infrastructure relative to nitrogen dispersal patterns. In this study, kelp lines were positioned north and northeast of the salmon pens to align with dominant current directions and enhance nutrient interception. However, finer-scale hydrodynamic modelling, such as that described by Broch et al. (2020), could improve placement strategies by resolving local flow dynamics and nutrient transport and fate with greater accuracy. Such models could also inform whether kelp should be concentrated in specific zones or distributed more broadly to capture waste transported over longer distances within the bay, taking more of a regional IMTA approach (Sanz-Lazaro and Sanchez-Jerez, 2020). Ultimately, the modelling framework presented here identifies the scale of cultivation required to reach a modest nitrogen removal target. A key next step is to better understand nitrogen movement across spatial and temporal gradients in the bay. While model refinement is one path forward, validation through direct measurements of dissolved inorganic nitrogen (DIN) uptake and retention, though challenging (Jansen et al., 2016), remains essential for evaluating bioremediation efficacy in real systems.

6. Conclusion

The modelled production scenarios in this study suggest that kelp growth at this salmon-kelp IMTA site would not be limited by nitrogen availability, with other environmental factors such as light playing a more significant role. Timing of kelp stocking was the most important factor among the scenarios investigated, and the results suggest that stocking kelp earlier (in autumn rather than winter) would improve yield and nitrogen uptake. Furthermore, the model approach also suggests that the number of kelp lines would have to increase in all scenarios to achieve a 10 % reduction in salmon-derived nitrogen waste, but significant kelp farm expansion may raise other logistical challenges. Overall, based on the results, optimisation of this salmon-kelp IMTA system would depend more on the strategies employed for planning kelp production rather than adjusting salmon production. Clearly, IMTA has many considerations, but this study has shown that this integrated modelling approach can provide useful information to support management of different species.

CRediT authorship contribution statement

Amalia Krupandan: Writing – original draft, Visualization, Validation, Software, Project administration, Methodology, Investigation, Formal analysis, Data curation, Conceptualization. **Lynne Falconer:** Writing – review & editing, Supervision. **Julie Maguire:** Writing – review & editing, Resources. **Trevor Telfer:** Writing – review & editing, Supervision, Funding acquisition, Conceptualization.

Funding

This work was completed under the EATFISH project. EATFISH is a Marie Skłodowska–Curie Actions Innovative Training Network funded by the EU (project number 956697).

Declaration of competing interest

The authors declare that they have no known competing financial interests or personal relationships that could have appeared to influence the work reported in this paper.

Acknowledgements

Nutritional Analytical Services at the University of Stirling for fatty acid analysis of salmon feed. MOWI Ireland for provision of salmon farm production data. Ana Nobre and Andreia Raposo at SPAROS for their support in the application of FEEDNETICS.

Appendix A. Supplementary data

Supplementary data to this article can be found online at https://doi.org/10.1016/j.aquaculture.2025.743299.

Data availability

Model code can be made available on request.

Data relating to publication: Salmon cage wastes increase kelp growth in commercial scale open coast integrated multi-trophic aquaculture system (Original data) (Zenodo)

References

Alexander, K.A., Hughes, A.D., 2017. A problem shared: technology transfer and development in European integrated multi-trophic aquaculture (IMTA). Aquaculture 473, 13–19. https://doi.org/10.1016/j.aquaculture.2017.01.029.

Azevedo, I.C., Duarte, P.M., Marinho, G.S., et al., 2019. Growth of *Saccharina latissima* (Laminariales, Phaeophyceae) cultivated offshore under exposed conditions. Phycologia 58, 504–515. https://doi.org/10.1080/00318884.2019.1625610.

Bannister, J., Sievers, M., Bush, F., Bloecher, N., 2019. Biofouling in marine aquaculture: a review of recent research and developments. Biofouling 35, 631–648. https://doi.org/10.1080/08927014.2019.1640214.

Borchers, H.W., 2011. pracma: Practical Numerical Math Functions. 2.4.4.

Bord Iascaigh Mhara, 2023. Irish Macro-Algal Cultivation Strategy to 2030. Review of the Irish Seaweed Aquaculture Sector and Strategy for Its Development to 2030.

Brager, L.M., Cranford, P.J., Jansen, H., Strand, Ø., 2016. Temporal variations in suspended particulate waste concentrations at open-water fish farms in Canada and Norway. Aquac. Environ. Interact. 8, 437–452. https://doi.org/10.3354/aei00190.

Broch, O., Ellingsen, I., Forbord, S., et al., 2013. Modelling the cultivation and bioremediation potential of the kelp *Saccharina latissima* in close proximity to an exposed salmon farm in Norway. Aquac. Environ. Interact. 4, 187–206. https://doi.org/10.3354/aei00080.

Broch, O.J., Slagstad, D., 2012. Modelling seasonal growth and composition of the kelp Saccharina latissima. J. Appl. Phycol. 24, 759–776. https://doi.org/10.1007/s10811-011-9695-y.

Broch, O.J., Klebert, P., Michelsen, F.A., Alver, M.O., 2020. Multiscale modelling of cage effects on the transport of effluents from open aquaculture systems. PLoS One 15, e0228502. https://doi.org/10.1371/journal.pone.0228502.

Bruhn, A., Tørring, D., Thomsen, M., et al., 2016. Impact of environmental conditions on biomass yield, quality, and bio-mitigation capacity of *Saccharina latissima*. Aquac. Environ. Interact. 8, 619–636. https://doi.org/10.3354/aei00200.

Cerca, M., Sosa, A., Vance, C., et al., 2024. Small-scale low-tropic ocean farming and coastal rural landscapes: why the logistics of seaweed matter? Insights from Ireland for collaborative planning. Mar. Policy 163, 106140. https://doi.org/10.1016/j.marpol.2024.106140.

Chary, K., Aubin, J., Sadoul, B., et al., 2020. Integrated multi-trophic aquaculture of red drum (*Sciaenops ocellatus*) and sea cucumber (*Holothuria scabra*): assessing bioremediation and life-cycle impacts. Aquaculture 516, 734621. https://doi.org/10.1016/j.aquaculture.2019.734621.

Chopin, T., Buschmann, A.H., Halling, C., et al., 2001. Integrating seaweeds into marine aquaculture systems: a key toward sustainability. J. Phycol. 37, 975–986. https://doi.org/10.1046/j.1529-8817.2001.01137.x.

Chopin, T., Cooper, J.A., Reid, G., et al., 2012. Open-water integrated multi-trophic aquaculture: environmental biomitigation and economic diversification of fed aquaculture by extractive aquaculture. Rev. Aquac. 4, 209–220. https://doi.org/10.1111/j.1753-5131.2012.01074.x.

Christensen, L.D., 2020. Seaweed cultivation in the Faroe Islands: analyzing the potential for forward and fiscal linkages. Mar. Policy 119, 104015. https://doi.org/10.1016/j.marpol.2020.104015.

Coleman, S., Gelais, A.T.S., Fredriksson, D.W., et al., 2022. Identifying scaling pathways and research priorities for kelp aquaculture nurseries using a techno-economic modeling approach. Front. Mar. Sci. 9. https://doi.org/10.3389/fmars.2022.894461.

Dabrowski, T., Lyons, K., Nolan, G., et al., 2016. Harmful algal bloom forecast system for SW Ireland. Part I: description and validation of an operational forecasting model. Harmful Algae 53, 64–76. https://doi.org/10.1016/j.hal.2015.11.015.

Ding, X., Brussaard, C.P.D., Timmermans, K.R., 2025a. Effects of elevated temperature on erosion of *Saccharina latissima* (Laminariales, sugar kelp) blades. J. Exp. Mar. Biol. Ecol. 582, 152071. https://doi.org/10.1016/j.jembe.2024.152071.

Ding, X., Soetaert, K., Timmermans, K., 2025b. Effect of temperature on growth and nitrate and phosphate uptake kinetics of juvenile *Saccharina latissima* sporophytes (Phaeophyceae). J. Appl. Phycol. https://doi.org/10.1007/s10811-025-03475-3.

Dumas, A., France, J., Bureau, D., 2010. Modelling growth and body composition in fish nutrition: where have we been and where are we going? Aquac. Res. 41, 161–181. https://doi.org/10.1111/j.1365-2109.2009.02323.x.

Falconer, L., Cutajar, K., Krupandan, A., et al., 2023. Planning and licensing for marine aquaculture. Rev. Aquac. 15, 1374–1404. https://doi.org/10.1111/raq.12783.

Fieler, R., Greenacre, M., Matsson, S., et al., 2021. Erosion dynamics of cultivated kelp, *Saccharina latissima*, and implications for environmental management and carbon sequestration. Front. Mar. Sci. 8. https://doi.org/10.3389/fmars.2021.632725.
Forbord, S., Etter, S.A., Broch, O.J., et al., 2021. Initial short-term nitrate uptake in juvenile, cultivated *Saccharina latissima* (Phaeophyceae) of variable nutritional state. Aquat. Bot. 168, 103306. https://doi.org/10.1016/j.aquabot.2020.103306.
Fossberg, J., Forbord, S., Broch, O.J., et al., 2018. The potential for upscaling kelp (*Saccharina latissima*) cultivation in Salmon-driven integrated multi-trophic aquaculture (IMTA). Front. Mar. Sci. 5, 418. https://doi.org/10.3389/fmars.2018.00418.
Gerard, V.A., 1987. Hydrodynamic streamlining of *Laminaria saccharina* Lamour. in response to mechanical stress. J. Exp. Mar. Biol. Ecol. 107, 237–244. https://doi.org/10.1016/0022-0981(87)90040-2.
Gordillo, F.J.L., 2012. Environment and algal nutrition. In: Wiencke, C., Bischof, K. (Eds.), Seaweed Biology. Springer, Berlin Heidelberg, Berlin, Heidelberg, pp. 67–86.
Hadley, S., Wild-Allen, K., Johnson, C., Macleod, C., 2015. Modeling macroalgae growth and nutrient dynamics for integrated multi-trophic aquaculture. J. Appl. Phycol. 27, 901–916. https://doi.org/10.1007/s10811-014-0370-y.
Hamby, D.M., 1994. A review of techniques for parameter sensitivity analysis of environmental models. Environ. Monit. Assess. 32, 135–154. https://doi.org/10.1007/BF00547132.
Handå, A., Forbord, S., Wang, X., et al., 2013. Seasonal- and depth-dependent growth of cultivated kelp (*Saccharina latissima*) in close proximity to salmon (*Salmo salar*) aquaculture in Norway. Aquaculture 414–415, 191–201. https://doi.org/10.1016/j.aquaculture.2013.08.006.
Hossain, A., Senff, P., Glaser, M., 2022. Lessons for coastal applications of IMTA as a way towards sustainable development: a review. Appl. Sci. 12, 11920. https://doi.org/10.3390/app122311920.
Hughes, A.D., Black, K.D., 2016. Going beyond the search for solutions: understanding trade-offs in European integrated multi-trophic aquaculture development. Aquac. Environ. Interact. 8, 191–199. https://doi.org/10.3354/aei00174.
Hurd, C.L., Harrison, P.J., Bischof, K., Lobban, C.S., 2014. Seaweed Ecology and Physiology, 2nd edn. Cambridge University Press.
Hvas, M., Kolarevic, J., Noble, C., et al., 2024. Fasting and its implications for fish welfare in Atlantic salmon aquaculture. Rev. Aquac. 16, 1308–1332. https://doi.org/10.1111/raq.12898.
Jansen, H.M., Reid, G.K., Bannister, R.J., et al., 2016. Discrete water quality sampling at open-water aquaculture sites: limitations and strategies. Aquac. Environ. Interact. 8, 463–480. https://doi.org/10.3354/aei00192.
Kleitou, P., Kletou, D., David, J., 2018. Is Europe ready for integrated multi-trophic aquaculture? A survey on the perspectives of European farmers and scientists with IMTA experience. Aquaculture 490, 136–148. https://doi.org/10.1016/j.aquaculture.2018.02.035.
Koch, S.J.I., Filgueira, R., Alberg, J., et al., 2024. Identifying an Optimal Operating Window for Seaweed Aquaculture: Balancing Expansion Barriers and Carrying Capacity.
Lavaud, R., Filgueira, R., Nadeau, A., et al., 2020. A dynamic energy budget model for the macroalga *Ulva lactuca*. Ecol. Model. 418, 108922. https://doi.org/10.1016/j.ecolmodel.2019.108922.
Lubsch, A., Timmermans, K.R., 2019. Uptake kinetics and storage capacity of dissolved inorganic phosphorus and corresponding dissolved inorganic nitrate uptake in *Saccharina latissima* and *Laminaria digitata* (Phaeophyceae). J. Phycol. 55, 637–650. https://doi.org/10.1111/jpy.12844.
McGrath, T., McGovern, E., Gregory, C., Cave, R.R., 2019. Local drivers of the seasonal carbonate cycle across four contrasting coastal systems. Reg. Stud. Mar. Sci. 30, 100733. https://doi.org/10.1016/j.rsma.2019.100733.
McKee, D., Cunningham, A., Dudek, A., 2007. Optical water type discrimination and tuning remote sensing band-ratio algorithms: application to retrieval of chlorophyll and *Kd*(490) in the Irish and Celtic seas. Estuar. Coast. Shelf Sci. 73, 827–834. https://doi.org/10.1016/j.ecss.2007.03.028.
Mock, T.S., Francis, D.S., Jago, M.K., et al., 2021. Seasonal effects on growth and product quality in Atlantic salmon fed diets containing terrestrial oils as assessed by a long-term, on-farm growth trial. Aquac. Nutr. 27, 477–490. https://doi.org/10.1111/anu.13200.
NASA Ocean Biology Processing Group, 2022. NOAA-20 VIIRS Level 3 Mapped Photosynthetically Available Radiation Data, Version R2022.0.
Nederlof, M.A.J., Verdegem, M.C.J., Smaal, A.C., Jansen, H.M., 2022. Nutrient retention efficiencies in integrated multi-trophic aquaculture. Rev. Aquac. 14, 1194–1212. https://doi.org/10.1111/raq.12645.
Nobre, A.M., Valente, L.M.P., Conceição, L., et al., 2019. A bioenergetic and protein flux model to simulate fish growth in commercial farms: application to the gilthead seabream. Aquac. Eng. 84, 12–22. https://doi.org/10.1016/j.aquaeng.2018.11.001.
Reid, G.K., Chopin, T., Robinson, S.M.C., et al., 2013. Weight ratios of the kelps, *Alaria esculenta* and *Saccharina latissima*, required to sequester dissolved inorganic nutrients and supply oxygen for Atlantic salmon, *Salmo salar*, in integrated multi-trophic aquaculture systems. Aquaculture 408–409, 34–46. https://doi.org/10.1016/j.aquaculture.2013.05.004.
Reid, G.K., Lefebvre, S., Filgueira, R., et al., 2020. Performance measures and models for open-water integrated multi-trophic aquaculture. Rev. Aquac. 12, 47–75. https://doi.org/10.1111/raq.12304.
Reynolds, P.J., 2005. Investigation of the Growth Potential and Ecosystem Impact of Intensively Farmed Atlantic Salmon Fed on Experimental Diets.
Roleda, M.Y., Hurd, C.L., 2019. Seaweed nutrient physiology: application of concepts to aquaculture and bioremediation. Phycologia 58, 552–562. https://doi.org/10.1080/00318884.2019.1622920.
Saltelli, A. (Ed.), 2008. Global Sensitivity Analysis: the Primer. John Wiley, Chichester, England Hoboken, NJ.
Sanz-Lazaro, C., Sanchez-Jerez, P., 2020. Regional integrated multi-trophic aquaculture (RIMTA): spatially separated, ecologically linked. J. Environ. Manag. 271, 110921. https://doi.org/10.1016/j.jenvman.2020.110921.
Sharma, S., Neves, L., Funderud, J., et al., 2018. Seasonal and depth variations in the chemical composition of cultivated *Saccharina latissima*. Algal Res. 32, 107–112. https://doi.org/10.1016/j.algal.2018.03.012.
Sickander, O., Filgueira, R., 2022. Factors affecting IMTA (integrated multi-trophic aquaculture) implementation on Atlantic Salmon (*Salmo salar*) farms. Aquaculture 561, 738716. https://doi.org/10.1016/j.aquaculture.2022.738716.
Soares, F.M.R.C., Nobre, A.M.D., Raposo, A.I.G., et al., 2023. Development and application of a mechanistic nutrient-based model for precision fish farming. J Mar Sci Eng 11, 472. https://doi.org/10.3390/jmse11030472.
Soetaert, K., Petzoldt, T., Setzer, R.W., 2008. deSolve: Solvers for Initial Value Problems of Differential Equations ("ODE", "DAE", 'DDE'). 1.40.
Son, S., Wang, M., 2015. Diffuse attenuation coefficient of the photosynthetically available radiation *Kd*(PAR) for global open ocean and coastal waters. Remote Sens. Environ. 159, 250–258. https://doi.org/10.1016/j.rse.2014.12.011.
Sprague, M., Fawcett, S., Betancor, M.B., et al., 2020. Variation in the nutritional composition of farmed Atlantic salmon (*Salmo salar* L.) fillets with emphasis on EPA and DHA contents. J. Food Compos. Anal. 94, 103618. https://doi.org/10.1016/j.jfca.2020.103618.
Stévant, P., Rebours, C., 2021. Landing facilities for processing of cultivated seaweed biomass: a Norwegian perspective with strategic considerations for the European seaweed industry. J. Appl. Phycol. 33, 3199–3214. https://doi.org/10.1007/s10811-021-02525-w.
Stévant, P., Marfaing, H., Rustad, T., et al., 2017. Nutritional value of the kelps *Alaria esculenta* and *Saccharina latissima* and effects of short-term storage on biomass quality. J. Appl. Phycol. 29, 2417–2426. https://doi.org/10.1007/s10811-017-1126-2.
Strain, P.M., Hargrave, B.T., 2005. Salmon aquaculture, nutrient fluxes and ecosystem processes in southwestern New Brunswick. In: Hargrave, B.T. (Ed.), Environmental Effects of Marine Finfish Aquaculture. Springer, Berlin, Heidelberg, pp. 29–57.
Veenhof, R.J., Burrows, M.T., Hughes, A.D., et al., 2024. Sustainable seaweed aquaculture and climate change in the North Atlantic: challenges and opportunities. Front. Mar. Sci. 11. https://doi.org/10.3389/fmars.2024.1483330.
Venolia, C.T., Lavaud, R., Green-Gavrielidis, L.A., et al., 2020. Modeling the growth of sugar kelp (*Saccharina latissima*) in aquaculture systems using dynamic energy budget theory. Ecol. Model. 430, 109151. https://doi.org/10.1016/j.ecolmodel.2020.109151.
Wang, X., Blikra, M.J., Evensen, T.H., et al., 2022. Effects of site, depth and sori origin on the growth and minerals composition of cultivated *Saccharina latissima* (Phaeophyceae) in the north of Norway. J. Appl. Phycol. 34, 529–541. https://doi.org/10.1007/s10811-021-02620-y.